Local Contractions Test Rigidity of E-Cadherin Adhesions

Yian Yang[1], Emmanuelle Nguyen[1], René-Marc Mège[2], Benoit Ladoux[1,2,*], Michael P. Sheetz[1,3,*]

[1]Mechanobiology Institute, National University of Singapore, Singapore 117411, Singapore

[2]Institut Jacques Monod (IJM), Université Paris Diderot, CNRS, UMR 7592, Paris 75013, France

[3]Department of Biological Sciences, Columbia University, New York, NY10027, USA

*Correspondence :

Michael P. Sheetz, ms2001@columbia.edu

Benoit Ladoux, benoit.ladoux@ijm.fr

Abstract

E-cadherin is a major cell-cell adhesion molecule involved in mechanotransduction at cell-cell contacts in tissues. Since epithelial cells respond to rigidity and tension in the tissue through E-cadherin, there must be active processes that test and respond to the mechanical properties of these adhesive contacts. Using sub-micrometer, E-cadherin-coated PDMS pillars, we find that cells generate active contractions between E-cadherin adhesions and pull to a constant distance for a constant duration, irrespective of varying pillar rigidities. These cadherin contractions require non-muscle myosin IIB, tropomyosin 2.1, α-catenin and binding of vinculin to α-catenin; plus, they are correlated with mechanosensitive cell spreading. Without contractions, cells fail to spread to different areas on soft and rigid surfaces and to maintain monolayer integrity. Thus, we suggest that epithelial cells test the rigidity of neighboring cells by cadherin contractions.

Introduction

For the proper organization of tissues, cells need to probe the mechanical properties of their micro-environment including extracellular matrix as well as neighboring cells through adhesive contacts. These mechanical properties are then transduced into biochemical information to regulate cell functions[1], including single and collective cell motility[2, 3], proliferation[4] or differentiation[5]. Of the many mechanical properties that cells control, stiffness appears to be an important parameter that is distinctive for a tissue and is reflected in the cells that constitute the tissue[6] . It follows that cells should be able to measure the stiffness of their neighbors to enable them to regulate their cell-cell contacts and cytoskeletal rigidity. Thus, it is important to understand how E-cadherin rigidity might be sensed. Recent studies have indeed found that epithelial cells spread to larger areas on rigid cadherin-coated surfaces than soft[7]. The testing of cadherin adhesion rigidity[8] shares similarities with the testing of matrix contact rigidity described for fibroblasts[9]. In the context of epithelial cell dynamics, this mechanism may allow cells to adapt to changes in the local stiffness of their neighbors due to cytoskeleton remodeling and reinforcement[10-12].

Cadherin rigidity is a complex mechanical parameter since it is defined as the force per unit area needed to displace a cadherin adhesion by a given distance. In the case of matrix rigidity sensing, cells pull matrix contacts to a constant deflection and measure the force generated[13-15]. The local matrix rigidity sensor is a sarcomere-like contraction complex (2 micrometers in length) that contracts matrix adhesions by 120 nm and if the force exceeds 25 pN, then a rigid-matrix signal is activated in the cell. The contractions are controlled by receptor tyrosine kinases in terms of the magnitude of deflection, the duration and the activation of the contractions[16, 17]. The sarcomere-like contraction system consists of antiparallel actin filaments anchored by α-actinin, a bipolar myosin filament and a number of actin binding proteins including tropomyosin 2.1[14, 15]. Although there are many obvious differences between cadherin and integrin adhesions[18], a similar

mechanism may be used to sense the rigidity of the E-cadherin contacts, i.e. neighboring cells.

Integrin and cadherin adhesions have many features in common, including an organization involving distinct nanometer-sized clusters of adhesion molecules[19, 20] and many actin-binding proteins[18]. In tissues, cadherin clusters form homophilic interactions that maintain adhesions between cells[21] and mechanically hold the tissue together. As primary components of adhesive contacts, cadherins are major parts of the mechanotransducing systems between cells[22, 23], and are important for tissue morphology [24]. Many cytoplasmic proteins link these adhesions to the cytoskeleton and provide mechanical continuity across the cell through a dynamic actomyosin network and other filamentous elements[25]. In addition, a "sarcomeric belt" structure was reported at apical cell-cell boundaries of epithelial cells, with non-muscle myosin II-mediated actomyosin structures interpolated in between cadherin clusters at a constant spacing[26, 27]. Other mechanical activities of epithelial monolayers also appear to involve actin and myosin contractions of the cadherin adhesions including the formation of cell-cell contacts[28], the contraction and bending of cell monolayers[27, 29] and tissue extension. The cadherin adhesion complexes are consequently a major element in mechanosensing events that ultimately shape the tissue and are involved in rigidity sensing and many other processes.

Previous studies have shown that cells generated high forces on large N-cadherin-coated pillars through cellular level contractions that were similar but not identical to matrix traction forces[8, 31]. N-cadherin-junctions that formed on N-cadherin-coated pillar surfaces resembled the morphology and dynamics of native epithelial cell–cell junctions[8]. Moreover, substrate stiffness modulated the level of force on E-cadherin adhesions that correlated with changes in cell spread area[7]. If the cadherin-based rigidity-sensing module was similar to the integrin-based sensor, then it should be evident in the deflection patterns of submicrometer diameter pillars[9]. When we placed E-cadherin expressing cells on submicrometer E-cadherin-pillars, we observed local contractile units of about 1-2.5 micrometers that pulled E-cadherin junctions together to a constant

distance of 130 nm, independent of rigidity over a 20-fold range. Unlike the integrin-based contractions, E-cadherin contractions did not require myosin IIA but were rather dependent upon myosin IIB, and also involved tropomyosin 2.1. E-Cadherin contractions required α-catenin and vinculin that were involved in linking E-cadherin to the actin cytoskeleton. The density of cadherin contractions correlated with the area of cells on cadherin surfaces, which was consistent with the increased spreading of MDCK cells on stiffer E-cadherin surfaces. Thus, we suggest that cells create local contraction units that pull between E-cadherin contacts to test rigidity properties of neighboring cells.

Results

Cos-7 and MDCK cells form contractile units on E-cadherin-coated pillars

Since previous studies indicated that E-cadherin clusters were spaced at a distance of ~1.4 μm[28], we prepared pillar substrates with a diameter of 600 nm and 1.2 μm center to center spacing. When pillars were coated with E-cadherin, cells attached and developed force on the pillars. To characterize E-cadherin-dependent force generation, we used Cos-7 cells, an SV-40 transformed derivative of African Green Monkey Kidney Fibroblasts, and Madin-Darby Canine Kidney (MDCK) epithelial cells. Cos-7 cells were of particular interest because these fibroblast-like cells expressed E-cadherin[32] while lacking a major myosin II isoform, Myosin IIA[33], that was needed to produce local contractions on fibronectin matrices[17]. Surprisingly, Cos-7 cells were able to adhere to, spread and pull on E-cadherin pillars and exhibited localized contractions (Fig. 1A, left panel). The spreading and force generation were similar to earlier studies using large cadherin-coated pillars[8, 34]; however, unlike the case with cells on the larger pillars, these sub-micrometer pillars revealed local contraction units of 1-2 micrometers like those previously found for integrin-based adhesions[9]. The criterion for the local contractions was that pairs of pillars moved toward each other for a limited period and maximum displacements occurred at approximately the same time point (see description below). When Cos-7 cells spread on E-cadherin coated pillars, there were many examples of local contractions (Fig. 1A, right panel), which were not observed with larger pillars before, indicating that these smaller pillars were able to reveal local contractions in addition to the radial contractions.

In general, it was difficult to separate all local contractile units from radial contractions because multiple contractile units often overlapped resulting in complex pillar displacements. Although some local contractions were not recorded, we used the very stringent requirement for pairs that two pillars move toward each other and relax at the same time. We characterized pulling-relaxing events of pillars by two parameters: D_{max}, maximum deflection value as the largest pillar displacement from the original position; and $T_{1/2}$, half-peak contraction time as the length of time that the pillar was pulled farther than half of the D_{max} value in a single pulling event (indicated in Fig. 1B). For computer identification of pillar pairs, we had two major criteria: 1) two pillars moved toward each other for more than 8s during deflections of greater than half the D_{max}, and 2) the D_{max} of both pillars occurred within 5s. After analyzing the time course of pillar movements under spreading cells for ~30 minutes, there was a significant density of local contractile units, in which pillars deflected and relaxed in a synchronized manner (Fig. 1B, local contractions were noted by dotted line-circled pillars in Fig.1A). Characterization of the contractile units provided a quantitative analysis of the local contractions and we designated those paired E-cadherin adhesion-dependent contractile events as "**c**adherin **c**ontractions" (CC). Although there were other pillar movements that could have been driven by local contractions but would not meet these strict criteria, we found a significant number of local contractions.

To determine if CCs were present in other cells, we chose MDCK epithelial cells. After spreading on E-cadherin pillars for 3 hours, they generated cadherin contractions in a similar fashion to Cos-7 cells (Supp. Fig. 1A). Analysis of the D_{max} of all pillar deflections showed that overall contractility much lower with Cos-7 cells than with MDCK cells owing to the absence of Myosin IIA in Cos-7 cells (Fig. 1C), while the magnitude of CC deflection was similar in both cell lines (Fig. 1D). These results supported the idea that CCs were generated in similar fashion and were a common event across different cell types in contrast to variations in overall force generation. Furthermore, analyses of the pillar deflections showed that the velocities of contraction

and relaxation were equal in CCs (Supp. Fig. 1B); whereas the contraction velocities were significantly higher than relaxation velocities for unpaired contractions in both MDCK and Cos-7 cells (Supp. Fig. 1C). We also suggest that the CC pairs were unlike integrin-dependent contractions because they formed in the absence of Myosin IIA. In contrast, large unpaired contractions were much less frequent in Cos-7 cells, indicating that high, unpaired deflections observed in MDCK cells were indeed powered by Myosin IIA.

Since the local CCs were distinct and highly regular both in the D_{max} and duration of contractions, we quantified the CC parameters under a variety of conditions, including different pillar rigidities. When MDCK cells were spread on pillars with different rigidities due to their different heights, the local CCs had very similar D_{max} values (Supp. Fig. 2A, 71.1±27.3 nm on 0.75 μm high pillars, and 66.9±20.2 nm on 1.5 μm high pillars that had spring constants of 95 pN/nm and 12 pN/nm, respectively), indicating that contraction distance was rigidity-independent as was previously observed for local matrix contractions[14, 15]. Similar features were observed for CCs of Cos-7 cells spreading on E-cadherin pillars (D_{max} of 59.6±24.0 nm on 0.75 μm high pillars, and of 60.9±24.6 nm on 2 μm high pillars that had spring constants of 95 pN/nm and 5 pN/nm) (Supp. Fig. 2B). Further, the average $T_{1/2}$ values were about 20.0 s for both Cos-7 and MDCK cells (Supp. Fig. 3A). These results further reinforced the idea that paired contractions were powered by the same process in MDCK and Cos-7 cells. Altogether, both MDCK and Cos-7 cells produced CCs that were independent of rigidity and had similar D_{max} and $T_{1/2}$ values. Thus, both MDCK and Cos-7 cells pulled to a constant deflection and then the force of the contractions was proportional to the rigidity.

E-cadherin-mediated rigidity response correlates with cadherin contraction density

The density of matrix contractions was indicative of rigidity-sensitive cell spreading[14, 17], and perhaps there was a similar correlation between CC density and spread area on E-cadherin-coated substrata. When MDCK cells spread on pillars coated with E-cadherin, cells spread to a larger area on stiff (~2 MPa) than on soft substrates (~5 kPa) and showed

more prominent polarization on stiff substrates (Fig. 2A and D). As predicted from the local matrix contractions, CC density in MDCK cells decreased with decreasing pillar rigidity (Fig. 2B, 5.41 CCs on 0.75 μm high pillars, 2.49 CCs on 1.5 μm high pillars, and 1.60 CCs on 2 μm high pillars on average). However, the density of Cos-7 CCs increased with decreasing pillar rigidity (Fig. 2C, 3.36 CCs on 0.75 μm high pillars and 6.38 CCs on 2 μm high pillars on average). This surprising result stimulated us to check the spreading of Cos7 cells on rigid and soft cadherin-coated surfaces. We observed that Cos7 cells spread to a larger area on soft (~5 pN/nm) than on rigid (~95 pN/nm) pillars (Fig. 2E), which correlated with higher CC density on soft pillars. These results indicated that CC formation was rigidity-sensitive and promoted cell spreading. However, Cos-7 cells did not respond to rigid cadherin in the same way as MDCK cells. Cos-7 cells exhibited transformed growth on soft fibronectin, which meant that they spread and grew equally well on soft and rigid fibronectin because they lacked rigidity-sensing contractions. Thus, the signal generated by CCs in Cos-7 cells may have been different than in MDCK cells.

α-catenin and vinculin co-operatively regulate cadherin contraction

To further investigate the role of cadherin adhesion proteins in CCs, we examined involvement of the major actin-binding proteins in the E-cadherin adhesions, α-catenin and vinculin. Previous studies showed that α-catenin was under force in the cadherin adhesion[35], and perhaps acted as a molecular mechanosensitive switch[36]. There was also evidence for involvement of vinculin in linking adhesion complexes to actin[37] that was consistent with its role as a force transducer. When MDCK cells stably missing α-catenin were placed on E-cadherin coated pillars, cadherin contraction density was greatly reduced (Fig. 3A). After α-catenin was restored in the knockdown cell line, a normal level of CCs was observed (Fig. 3B, paired CCs marked by green vectors) showing that α-catenin was critical in forming CCs (Fig. 3C). In addition, we also found that α-catenin knockdown reduced $T_{1/2}$ value and Dmax in the non-paired contractions, which could be restored through α-catenin rescue (Supp. Fig. 3B and C). These results indicated that α-catenin was a crucial component in CCs and was generally involved in linking cadherin

adhesions to the contractile cytoskeleton.

To determine if vinculin was also involved in CC formation, we tested vinculin depleted MDCK cells and characterized their CCs on pillars. We found that vinculin knockdown cells had a much lower density of CCs when compared with wild-type MDCK cells, while re-expression of vinculin restored CC density to normal levels (Fig. 3D). We also measured the effect of vinculin depletion on overall deflection magnitude and time duration of the non-paired contractions, but there was no significant difference in both parameters after vinculin knockdown (Supp. Fig. 4C-D). Thus, vinculin's presence was necessary for the normal CC density, but vinculin depletion had no observed effect on overall cell contractility.

We next tested whether the association of vinculin with α-catenin was important. Although vinculin's role in regulating force generation remained unclear, the interaction between vinculin and α-catenin depended upon the unfolding of α-catenin[36, 38] . To test if α-catenin-vinculin binding affinity affected cadherin contraction, we rescued α-catenin knockdown MDCK cells with an α-catenin mutant L344P that did not bind vinculin[39]. Upon L344P mutant rescue, local CC density was also significantly reduced compared with wild-type cells (Fig. 3C). Thus, the interaction between vinculin and α-catenin appeared to be important for CC formation.

To further investigate the role of CC activity of MDCK cells in cell spreading, wild-type cells as well as α-catenin or vinculin depleted cells were spread on soft and rigid E-cadherin surfaces. We observed that wild-type MDCK cells spread more on rigid than on soft substrates, in agreement with previous results on pillars with varying stiffness (Fig. 2D, Fig. 3E). When cells lost ability to form cadherin contractions due to α-catenin or vinculin depletion, the cells spread similarly on soft and stiff substrates. In both cases, depleted cells spread less on the 2 MPa rigid substrate than wild-type cells (Fig. 3E). This was consistent with the hypothesis that CCs were involved in stabilizing the spread state

and they required α-catenin and vinculin to form.

Since both α-catenin and vinculin were indispensable in CC formation, we next tested the possibility that failure in CC formation would alter organization of cell monolayers. We seeded MDCK cells and let them grow to confluency for 2 days. 3D reconstruction of confocal images of actin showed that compared with the uniform monolayers formed by wild-type cells (Supp. Fig. 5A), α-catenin and vinculin knockdown cells formed abnormally organized monolayers, with protruding cells and less organized actin (Fig. 4A). 3D imaging of E-cadherin and actin organization in confluent monolayers showed that α-catenin knockdown induced formation of protruding cell aggregates above the basal monolayer, with actin and E-cadherin remaining localized at cell-cell boundaries (Supp. 5B). In comparison, vinculin knockdown cells had disorganized actin areas, and E-cadherin failed to properly localize at cell-cell boundaries as well (Supp. Fig. 5C). When we quantified the area of protruding cells above basal monolayer through analysis of actin staining distribution, we found that both α-catenin and vinculin knockdown cells had a significantly greater area protruding above cell monolayer than wild-type cells (Fig. 4B). We also performed a wound healing assay, and we observed that α-catenin knockdown retarded cell migration rate significantly, and vinculin knockdown reduced migration rate mildly (Fig. 4C, Supp. Fig. 5D). These phenotypes correlated with depletion of CCs and indicated that CCs may have a role in maintaining normal epithelial integrity and collective cell migration.

Myosin IIB and Tpm2.1 mediate cadherin contraction

When MDCK cells spread on E-cadherin-coated pillar arrays, they were able to form individual E-cadherin clusters on pillar tips, but phosphorylated myosin light chain (pMLC) was found between E-cadherin clusters (Supp. Fig. 6A). This resembled fibroblast spreading on fibronectin-coated pillars in that integrins concentrated on pillars whereas pMLC was in between[9]. We also observed that treatment with Y-27632, a Rho-associated protein kinase (ROCK) inhibitor, fully abolished CC formation in Cos-7 cells (Supp. Fig. 6B). These results indicated that myosin activity was critical for CC

formation.

Previous studies indicated that all three types of non-muscle myosin II activity were involved in E-cadherin contact dynamics[27, 40] and E-cadherin-based force generation[8]. However, Cos-7 cells lacked non-muscle Myosin IIA and expressed primarily Myosin IIB plus a minor fraction of Myosin IIC[33]. Since the CC density was similar in Cos-7 and MDCK cells, it was unlikely that Myosin IIA was involved in CCs. To determine whether Myosin IIB or Myosin IIC were involved in CCs, we immunostained Cos-7 cells spread on E-cadherin substrata for Myosin IIB and Myosin IIC. Myosin IIB immunostaining co-localized with pMLC at the cell edge, where most of the CCs were found (Supp. Fig. 6C). In contrast, Myosin IIC did not localize with CCs in spread Cos-7 cells and did not co-localize with pMLC (Supp. Fig. 6D). At a super-resolution level, phosphorylated myosin IIB bipolar minifilaments localized between two contracting pillars (Fig. 5A), suggesting direct involvement of Myosin IIB in CC formation. To confirm that myosin IIB was indispensable in CC formation, we knocked down myosin IIB with shRNA and introduced myosin IIA-GFP in Cos-7 cells at the same time to create myosin IIA positive, IIB negative Cos-7 cells (Fig. 5B). We found that these cells had many fewer CCs than did normal Cos-7 cells (Fig. 5C), confirming that Myosin IIB, rather than IIA or IIC, was involved in CCs.

Tropomyosin (Tpm) was identified as a major component in integrin contractile units, and cells were incapable of forming contractions or sensing rigidity when Tpm2.1 protein levels were downregulated[14]. Recent discoveries have indicated that several types of tropomyosin, notably Tpm2.1 and Tpm3, were involved in E-cadherin adhesion integrity[41, 42]. We found that Tpm2.1 accumulated in between E-cadherin-coated pillars in newly spread areas where CCs formed in the periphery of Cos-7 cells, which resembled its localization in integrin contractile units [14]. However, staining of Tpm3 showed that it was much more centrally located in the cells and did not overlap with CC-abundant areas or Tpm2.1 (Supp. Fig. 7A). We also found that pMLC localized to Tpm2.1-rich regions at the cell periphery (Supp. Fig. 7B). Moreover, we found that CCs localized at Tpm2.1-

rich areas, where pMLC complexes were also observed to bridge between two contracting pillars (Supp. Fig. 7C). To confirm its involvement in CC formation, we knocked-down Tpm2.1 in Cos-7 cells (see loss of Tpm2.1 staining in kd cells, Supp. Fig. 7D). Tpm2.1 knockdown in Cos-7 cells resulted in drastically reduction of CC formation (Fig. 5D), indicating that Tpm2.1 played an important role in CC assembly.

Discussion

In this study, we find that paired contractions of E-cadherin coated pillars correlate with the ability of the cells to sense cadherin rigidity and to form epithelial monolayers. In the CCs, cells contract pillar pairs by 60-70 nm each with a halftime of the contractions of about 20 s irrespective of pillar rigidity over nearly a twenty-fold range of rigidity (from ~5 to ~100 kPa). As predicted from previous studies of the proteins in cadherin junctions, α-catenin, vinculin, myosin IIB and tropomyosin 2.1 were needed for the CC units (Fig. 6). Of the cadherin adhesion complex proteins, α-catenin and vinculin could anchor actin filaments to the adhesions. The CCs are distinct from local fibronectin matrix contractions in that they do not rely upon Myosin IIA but rather require Myosin IIB as well as α-catenin. Further, they are distinct from the unpaired, radial contractions of E-cadherin-coated pillars in length of deflection and velocity distribution. Because CC pairs form preferentially in newly spread areas of the cell, we suggest that they are primarily involved in new adhesion formation. Also, we find CC density to be rigidity sensitive since density increases with increasing rigidity in MDCK cells and decreases with increasing rigidity in Cos7 cells. Further, CC density changes correlate with changes in spread area on different rigidity cadherin surfaces. Thus, it seems that the CCs are important for the formation and maintenance of normal epithelia.

Local contractions between E-cadherin adhesions provide a simple mechanism for testing the rigidity of neighboring cells that is analogous to local matrix contractions to test matrix rigidity even though the details are distinct. Many physiological processes are

postulated to involve cadherin adhesion mechanosensing such as convergent extension [43] and epithelial tissue movements[44]. In those cases, monolayer morphology alteration is coupled with continued cell-cell sensing, and this indicates that there is a general mechanism of E-cadherin sensing in tissues[6]. Recent studies indicate that the rigidity of cadherin-coated surfaces affects cellular responses, indicating that the cells can sense cadherin rigidity[7, 8]; however, little is known regarding how cells employ force-generating molecular complexes to test rigidity through cadherin adhesions. The presence of the local contractions provides a simple mechanism for probing cell rigidity, because pulling cells contract to a constant distance and sense the force that is a simple measure of the rigidity of the cell contact. In a general context, although there is at this stage only a poor understanding of how contractile force is converted into a signal for rigidity, the similarity of the mechanism of sensing matrix rigidity to that of sensing cadherin rigidity is logical and could also be adapted for other aspects of cellular mechanics.

In the case of the cell-matrix rigidity sensing, the complex is similar to a sarcomere in terms of the components and the organization. Basically, anti-parallel actin filaments cover the 1.5-2.5 micrometer gap between matrix adhesions and myosin II bipolar filaments contract them at a very slow rate of 2-3 nm/s. Similarly, the CCs are driven by myosin II between two contact areas and the velocity of contractions is 2-3 nm/s. The major differences are in the type of myosin II with Myosin IIB powering CCs and Myosin IIA powering matrix contractions and in the primary cadherin complex proteins, α-catenin and vinculin, that anchor the actin filaments needed for CCs.

In terms of the mechanism of linkage with the actin cytoskeleton, the CCs depend strongly upon α-catenin and vinculin. Both proteins are involved in actin binding to the E-cadherin complex[10]. Knockdown of α-catenin reduces the number of contraction events. This indicates that α-catenin serves as an important mechanical linker between cadherin adhesion and actomyosin and α-catenin is an important component for force transmission at the cellular level. Similarly, depletion of vinculin causes a dramatic decrease in the density of CCs; in addition, decreasing the vinculin binding affinity of α-catenin also

reduces CCs. If vinculin binding is important for stable actin linkages to α-catenin[35, 45], then it is not surprising that alterations that weaken vinculin binding to α-catenin alter CC formation.

The role of α-catenin and vinculin in CC extended to their regulatory role in tissue integrity. α-catenin has been identified as a tumor suppressor, and its depletion could trigger YAP-1 mediated overgrowth[46]. Similarly, disruption of myosin-powered contractility also induced YAP-associated contact inhibition failure[47]. We observed that either α-catenin or vinculin knockdown caused disorder in cell monolayers. Further, depletion of vinculin significantly disrupts actin organization and E-cadherin localization at cell-cell boundary; however, depletion does not alter overall force generation behavior of cells in both magnitude and time duration (Supp. Fig. 4C-D) and only abolishes CC formation,. Thus, the effects of either α-catenin or vinculin knockdown clearly indicate that they have indispensable roles in CC formation and perhaps relatedly in tissue integrity maintenance.

Involvement of Tpm2.1 again highlighted that cadherin contractions and integrin contractions share key molecular components. As a common regulator of both rigidity sensing events, the role of Tpm2.1 in CC formation provides another insight in rigidity insensitivity of Tpm-deficient cancer cells. Besides their insensitivity to matrix rigidity, they might also not be able to test and respond to rigidity of neighboring cells due to the lack of cadherin contractions and would also not be able to respond properly to mechanical changes in the tissue. Previous studies also pointed out that Tpm2.1 knockdown in epithelial cells retarded wound closure[41], which agrees with our wound healing assay results in CC-deficient MDCK cells with α-catenin or vinculin knockdown. These results further support a significant role for Tpm2.1 in regulation of tissue integrity and cancer suppression through cadherin mechanotransduction, in addition to its role previously revealed in cell-matrix rigidity sensing[14].

The transient nature of the E-cadherin contraction units is consistent with the transient nature of many cellular mechanotesting processes[48]. Due to radically different effects of pillar rigidity on contractile unit density, the functions of contractile units may differ in different cell types. In the MDCK cells, the fact that contractile unit density decreases with lower pillar rigidity helps to explain the lower spread area on softer gels. Although we do not understand why Cos-7 cells spread less on rigid surfaces, the density of the CCs correlates with the spread area. Since integrin contractile units help to reinforce adhesions, the lower number of cadherin contractions might also result in fewer stable adhesions and cause lower spread area. In an in vivo scenario, fewer CCs could lead to decreased intercellular tension and improper mechanical feedback from neighboring cells. The fact that MDCK cells were able to generate CCs after adhering to E-cadherin substrates for several hours indicates that CC formation may be continuous at cell-cell boundaries, enabling cells to mechanically monitor their neighbors in real-time. Thus, the ability of cells to "pinch" their neighbor's cadherin complexes and respond to the force generated can tell the cell about the physical state of its neighbor regarding cortical tension integrity. In addition, CCs are observed in cells with different physiological backgrounds, indicating that they have a ubiquitous role in probing the surrounding cells. Thus, characterization of cadherin contractions can provide a reliable assay of E-cadherin mediated mechanosensory events, to better understand the intercellular rigidity sensing mechanism.

Materials and methods

Cell lines and culture

All MDCK cell lines (ATCC) and Cos-7 cells (ATCC) were cultured in high-glucose, L-glutamine containing DMEM with 10% of fetal bovine serum (FBS). For all assays using E-cadherin coated surfaces, high-glucose, L-glutamine containing DMEM without FBS, and supplemented with 100U/mL penicillin/100μg/mL streptomycin was used in experiments. All reagents were from Thermofisher. MDCK cell lines (GFP- and mCherry-tagged E-cadherin) were acquired from W. J. Nelson's lab[49]. Stable knockdown of α-catenin in MDCK cells was performed with shRNA in W. J. Nelson lab[50]. The

Vinculin knockdown MDCK cell line was a generous gift from Dr. Jay Groves lab in MBI, originating from Dr. Soichiro Yamada's group in University of California, Davis[51]. Cos-7 cell line was from Dr. Michael Sheetz lab.

Plasmids and transfection

Non-muscle myosin IIB shRNA and vinculin-GFP plasmid was a gift from Dr. Alexander Bershadsky lab in MBI, vinculin-GFP originated from Michael Davidson lab in Florida State University. α-Catenin plasmids (wild-type and L344P mutant) and GFP-E-cadherin plasmids were described earlier[39]. Tpm2.1 knockdown was performed with siRNA oligonucleotides as previously published[14].

Neon® Transfection System (Thermo Fisher) was used for electroporation of MDCK cells. Lipofectamine 2000 (Thermo Fisher) was used for chemical transfection of Cos-7 cells.

Preparations of nanopillar arrays and flat gel substrates

We used sub-micron size pillars for recording and analyzing cell contraction behavior. The pillars were in a square pattern, 500nm in diameter (D), and with three different heights (L) in 750nm, 1500nm and 2000nm. Pillars were made by PDMS (Sylgard® 184 Silicone Elastomer Kit), mixed at a ratio of 10:1, spin-coated on silicon molds and cured at 80°C for 2 hours. For pillars of 600nm in diameter, bending stiffness was calculated to be ~95nN/μm for 750nm tall pillars and ~5nN/μm for 2000nm tall pillars, stiffness were quantified as previously published[9]. Pillars were patterned in a square grid, with neighboring centroid-to-centroid distance of 1.2μm (2D) or 2.4μm (4D). Flat PDMS gel surfaces were prepared on glass coverslips with Sylgard 184 silicone elastomer kit (Dow Corning). PDMS surfaces with a Young's modulus of 2MPa were made with elastomer to curing agent ratio of 10:1, and 5kPa surfaces were made with ratio of 75:1, as previously published [52].

For E-cadherin coating, PDMS films with polymerized pillars were peeled from silicon molds and stuck on the glass surface of 12 mm glass bottom dishes (Iwaki) and treated with plasma for 5 minutes before incubated with 10μg/ml anti-human Fc antibody

(Jackson research, goat anti human) in 0.1M borate buffer with pH=8 in 4°C overnight. For flat PDMS substrates, samples were treated by the same procedure without surface plasma treatment. Coated substrates were washed with DPBS three times, and reacted with 10μg/ml E-cadherin-Fc antibody (R&D systems, diluted in DPBS containing Mg^{2+} and $Ca^{2+)}$ for 2 hours in room temperature, and washed with DPBS three times before use.

Cell spreading assay, would healing assay, drug treatment and immunostaining

MDCK cells (wild-type and all knockdown lines) were trypsinized and replated onto E-cadherin coated pillar arrays at low density in serum-free media as mentioned above, and incubated at 37 ℃ for 3 hours for cells to properly adhere to pillars before transfer to the microscope for imaging. For spreading assays on PDMS gels, cells were replated onto E-cadherin coated PDMS gels at low density in serum-free media and incubate at 37 °C for 6 hours before fixation and staining. Cos-7 cells were trypsinized and replated onto E-cadherin coated pillars and imaged immediately since they started to spread in a rapid manner. For wound-healing assay, cells were cultured to near-confluent density in 35mm Petri Dish (Nunc), and then scratched at the central area of confluent cell monolayers. Cells were then plated in Biostation IMQ microscope (Nikon) for long-term imaging. For Y-27632 (Y0503, Sigma) treatment, Cos-7 cells were treated with 10μM Y-27632 for 2 hours, resuspended with drug-containing serum-free media and seeded onto pillar substrates for image acquisition.

For cell immunostaining in general, cells were fixed with 3.7% paraformaldehyde (PFA, diluted in DPBS containing Mg^{2+} and Ca^{2+}) for 15 minutes at 37 ℃, permeabilized with 0.1% Triton X-100 for 10 minutes at room temperature, and blocked with 1% bovine serum albumin (BSA)/DPBS solution (blocking buffer) for 1 hour before staining with primary antibody in blocking buffer at 4 °C overnight. Samples were washed four times with DPBS before secondary antibody staining in blocking buffer for 1 hour at room temperature and washed four times afterwards before DAPI staining for 5 minutes. Phalloidin staining was applied together with secondary antibody incubation for 1 hour.

Primary antibodies used in experiments are listed as following: Phospho-Myosin Light Chain 2 (Ser19, Mouse mAb #3675 and Rabbit mAb #3671, CST), non-muscle myosin IIA (M8064, Sigma), non-muscle myosin IIB (CMII 23, DSHB), non-muscle myosin IIC heavy chain (PRB-444P, Covance), Tpm2.1 (TM311, Sigma), Tpm3 (ab180813, Abcam), E-cadherin (610181, BD Biosciences).

Microscopy imaging and data analysis

Cell spreading on pillars was imaged with a DeltaVision system attached to an Olympus IX71 inverted microscope with x100 oil immersion objective (1.40NA, UPlanSApo) and Photometrics CoolSNAP HQ2 (CCD) camera. SoftWoRx (4.10) software was used to control imaging configuration and recording. Fluorescence imaging of cells on pillars or PDMS gels were acquired using a spinning-disc confocal microscope (PerkinElmer) attached to an Olympus IX81 inverted microscope. Super-resolution confocal images were acquired using Live-SR (Roper Scientific) module attached to a Nikon Eclipse Ti-E inverted Microscope body, controlled by MetaMorph (7.10.1.161), iLas (1.2.0) and Live-SR (1.7.3) software. Biostation IMQ (Nikon) was used to record wound healing process, cell samples were supplemented with 5% CO_2 and were imaged with 10x objective for up to 24 hours.

Pillar position detection was conducted in ImageJ (NIH) through tracking plugins designed by Dr. Felix Margadant. Pillar deflection analysis was conducted through Matlab (Math works), Statistical analysis and graph plotting were generated through Prism (Graphpad software), all bar plots were presented in Mean $\pm$ SEM. Cadherin contraction detection program was adapted from Matlab codes used in previous studies of integrin contractile units[17]. Analyses of significant difference levels were performed using unpaired Student's t-test with Welch's correction.

Acknowledgements

We thank all the members of the Sheetz and Mège-Ladoux labs for their help, especially F. Margadant, S. Liu and B. Yang for their help in designing ImageJ plugins and Matlab codes for pillar analysis. We thank the Core Facilities of Mechanobiology Institute. Y. Yang and E. Nguyen are supported by Mechanobiology Institute, National University of Singapore and Ministry of Education, Singapore. R.-M. Mège is supported by Fondation ARC, Projet International de Coopération Scientifique (PICS) CNRS programmes, France-Singapour exchange grant, National University of Singapore-Université Sorbonne-Paris-Cité (NUS-SPC) exchange grant and Fondation pour la Recherche Médicale (FRM). B. Ladoux is supported by Mechanobiology Institute, the European Research Council under the European Union's Seventh Framework Program (FP7/2007-2013) / ERC grant agreements n° 617233, Agence Nationale de la Recherche (ANR) "POLCAM" (ANR-17- CE13-0013) and USPC-NUS program. M. P. Sheetz is supported by NIH grants, NUS grants and Mechanobiology Institute, National University of Singapore.

Author Contributions

Y.Y. and E.N. performed the experiments; Y.Y. analyzed the data; B.L. and M.P.S. designed the study; Y.Y., R.-M.M., B.L. and M.P.S. wrote and prepared the manuscript.

Competing financial interests

The authors declare no competing financial interests.

Figure Legends

Figure 1. Cell generates local contractile units on E-cadherin coated pillars.
A) Left: pillar deflection vector map under a Cos-7 cell. Red vectors indicate non-paired deflections, green vectors indicate paired deflections, grey line indicates cell boundary. Scale bar 5μm. Right: Amplification of contraction-generation cell spreading area. Scale bar 2μm. B) Deflection plot of paired pillars under one contraction event, correlated with pillars indicated in A) in yellow dotted line circle. C) Histogram plots of overall D_{max} distribution of MDCK cells and Cos-7 cells, dotted lines show mean D_{max} value of MDCK and Cos-7 cells in respective color. D_{max}=72.6±45.8nm for MDCK cells, and 31.7±20.1nm for Cos-7 cells. D) Histogram plots of paired deflection D_{max} distributions in MDCK cells and Cos-7 cells. D_{max}=71.1±27.3nm for MDCK cells, and 59.6±24.0nm for Cos-7 cells.

Figure 2. CC density correlates with cell spreading area on E-cadherin.
MDCK cell spreading on PDMS surfaces coated with E-cadherin, with stiffness of 2MPa (left) and 5kPa (right). Scale bar 10μm. B) Bar plots of CC density of MDCK cells spreading on pillars with stiffnesses of 95 and 5pN/nm. C) Bar plots of CC density of Cos-7 cells spreading on E-cadherin coated pillars with stiffnesses of 95 and 5pN/nm. D) Box-and-Whisker Plots of spreading area of MDCK cells on E-cadherin coated pillars with stiffnesses of 95 and 5pN/nm. E) Box-and-Whisker Plots of spreading area of Cos-7 cells on E-cadherin coated pillars with stiffnesses of 95 and 5pN/nm. (*$p<0.05$, **$p<0.01$)

Figure 3. Depletion of α-catenin and vinculin in MDCK cells alters generation of CCs.
Vector map of pillar deflection under A) α-catenin knockdown and B) α-catenin-rescued knockdown cell. Red vectors indicate non-paired deflections, green vectors indicate paired deflections. Yellow line indicates cell boundary. Scale bar 2μm. C) Bar plots of density of CCs generated by MDCK cells of wild type or with α-catenin knockdown, L344P mutated α-catenin rescue and wild-type α-catenin rescue. D) Bar plots of density of CCs generated by MDCK cells of wild-type, vinculin knockdown and rescue. (n=5 in

each case, *, $p<0.05$; ns, non-significant) E) Box-and-Whisker Plots of cell spreading area of wild type, α-catenin knockdown and vinculin knockdown MDCK cells on E-cadherin coated PDMS surfaces of 2MPa or 5kPa. (**, $p<0.01$; ns, non-significant)

Figure 4. Deficiency of CC formation in MDCK cells induces abnormal monolayer formation and retarded collective migration.

A) 3D reconstruction of actin (in red) in cell monolayers formed by wild-type (left panels), α-catenin knockdown (middle panels) or vinculin knockdown (right panels) MDCK cells. Upper panels show x-y views, lower panels show tilted 3D views. Scale bar 20μm. B) Bar plots of percentage of cell areas protruding above basal monolayers in wild-type, α-catenin knockdown and vinculin knockdown MDCK cell layers. (n=7 in each case, ***, $p<0.001$) B) Bar plots of wound healing speed of wild-type, α-catenin knockdown and vinculin knockdown MDCK cell monolayers. (n=6 in each case, **, $p<0.01$; ****, $p<0.0001$)

Figure 5. Non-muscle myosin IIB and Tpm2.1 mediates CC formation.

A) Immunostaining of pMLC (in green) and myosin IIB heavy chain (in red) in Cos-7 cell on E-cadherin pillars. Right panel shows phosphorylated myosin IIB mini-filament (shown in dotted line circle) between contracted pillars, deflections of which represented in orange arrows. Scale bar 5μm. B) Immunostaining of Myosin IIA and IIB in Cos-7 cells (wild-type & with Myosin IIA-GFP and Myosin IIB shRNA). Scale bar 10μm. C) Bar plots of CC density of Cos-7 cells (wild-type & with Myosin IIA-GFP and Myosin IIB shRNA) on E-cadherin pillars. (n=5 in each case, **, $p<0.01$) D) Bar plots of CC density of Cos-7 cells (wild-type & transfected with Tpm2.1 shRNA) on E-cadherin pillars. (n=5 in each case, **, $p<0.01$)

Figure 6. Schematic representation of molecular mechanism of Cadherin Contraction.

References

1. Vogel, V. & Sheetz, M. Local force and geometry sensing regulate cell functions. *Nat Rev Mol Cell Biol* **7**, 265-275 (2006).
2. Lo, C.M., Wang, H.B., Dembo, M. & Wang, Y.L. Cell movement is guided by the rigidity of the substrate. *Biophysical journal* **79**, 144-152 (2000).
3. Sunyer, R. *et al.* Collective cell durotaxis emerges from long-range intercellular force transmission. *Science (New York, N.Y.)* **353**, 1157-1161 (2016).
4. Wang, H.B., Dembo, M. & Wang, Y.L. Substrate flexibility regulates growth and apoptosis of normal but not transformed cells. *American journal of physiology. Cell physiology* **279**, C1345-1350 (2000).
5. Engler, A.J., Sen, S., Sweeney, H.L. & Discher, D.E. Matrix elasticity directs stem cell lineage specification. *Cell* **126**, 677-689 (2006).
6. Discher, D.E., Janmey, P. & Wang, Y.L. Tissue cells feel and respond to the stiffness of their substrate. *Science (New York, N.Y.)* **310**, 1139-1143 (2005).
7. Collins, C., Denisin, A.K., Pruitt, B.L. & Nelson, W.J. Changes in E-cadherin rigidity sensing regulate cell adhesion. *Proceedings of the National Academy of Sciences of the United States of America* **114**, E5835-e5844 (2017).
8. Ladoux, B. *et al.* Strength dependence of cadherin-mediated adhesions. *Biophysical journal* **98**, 534-542 (2010).
9. Ghassemi, S. *et al.* Cells test substrate rigidity by local contractions on submicrometer pillars. *Proceedings of the National Academy of Sciences of the United States of America* **109**, 5328-5333 (2012).
10. Ladoux, B., Nelson, W.J., Yan, J. & Mege, R.M. The mechanotransduction machinery at work at adherens junctions. *Integr Biol (Camb)* **10** 1109-1119 (2015).
11. Takeichi, M. Dynamic contacts: rearranging adherens junctions to drive epithelial remodelling. *Nat Rev Mol Cell Biol* **15**, 397-410 (2014).
12. Ladoux, B. & Mege, R.M. Mechanobiology of collective cell behaviours. *Nat Rev Mol Cell Biol* **18**, 743-757 (2017).
13. Saez, A., Buguin, A., Silberzan, P. & Ladoux, B. Is the Mechanical Activity of Epithelial Cells Controlled by Deformations or Forces? *Biophysical journal* **89**, L52-L54 (2005).
14. Wolfenson, H. *et al.* Tropomyosin controls sarcomere-like contractions for rigidity sensing and suppressing growth on soft matrices. *Nature cell biology* **18**, 33-42 (2016).
15. Meacci, G. *et al.* alpha-Actinin links extracellular matrix rigidity-sensing contractile units with periodic cell-edge retractions. *Molecular biology of the cell* **27**, 3471-3479 (2016).
16. Yang, B. *et al.* Mechanosensing Controlled Directly by Tyrosine Kinases. *Nano letters* **16**, 5951-5961 (2016).
17. Saxena, M. *et al.* EGFR and HER2 activate rigidity sensing only on rigid matrices. *Nature materials* **16**, 775-781 (2017).
18. Ladoux, B., Mege, R.M. & Trepat, X. Front-Rear Polarization by Mechanical Cues: From Single Cells to Tissues. *Trends in cell biology* **26**, 420-433 (2016).

19. Changede, R., Xu, X., Margadant, F. & Sheetz, M.P. Nascent Integrin Adhesions Form on All Matrix Rigidities after Integrin Activation. *Developmental cell* **35**, 614-621 (2015).
20. Wu, Y., Kanchanawong, P. & Zaidel-Bar, R. Actin-delimited adhesion-independent clustering of E-cadherin forms the nanoscale building blocks of adherens junctions. *Developmental cell* **32**, 139-154 (2015).
21. Niessen, C.M., Leckband, D. & Yap, A.S. Tissue organization by cadherin adhesion molecules: dynamic molecular and cellular mechanisms of morphogenetic regulation. *Physiological reviews* **91**, 691-731 (2011).
22. Leckband, D.E. & de Rooij, J. Cadherin adhesion and mechanotransduction. *Annual review of cell and developmental biology* **30**, 291-315 (2014).
23. Mege, R.M. & Ishiyama, N. Integration of Cadherin Adhesion and Cytoskeleton at Adherens Junctions. *Cold Spring Harb Perspect Biol* (2017).
24. Lecuit, T. & Yap, A.S. E-cadherin junctions as active mechanical integrators in tissue dynamics. *Nature cell biology* **17**, 533-539 (2015).
25. Moore, S.W., Roca-Cusachs, P. & Sheetz, M.P. Stretchy proteins on stretchy substrates: the important elements of integrin-mediated rigidity sensing. *Developmental cell* **19**, 194-206 (2010).
26. Ebrahim, S. *et al.* NMII forms a contractile transcellular sarcomeric network to regulate apical cell junctions and tissue geometry. *Current biology : CB* **23**, 731-736 (2013).
27. Choi, W. *et al.* Remodeling the zonula adherens in response to tension and the role of afadin in this response. *The Journal of cell biology* **213**, 243-260 (2016).
28. Engl, W., Arasi, B., Yap, L.L., Thiery, J.P. & Viasnoff, V. Actin dynamics modulate mechanosensitive immobilization of E-cadherin at adherens junctions. *Nature cell biology* **16**, 587-594 (2014).
29. Martin, A.C. & Goldstein, B. Apical constriction: themes and variations on a cellular mechanism driving morphogenesis. *Development (Cambridge, England)* **141**, 1987-1998 (2014).
30. Collinet, C., Rauzi, M., Lenne, P.F. & Lecuit, T. Local and tissue-scale forces drive oriented junction growth during tissue extension. *Nature cell biology* **17**, 1247-1258 (2015).
31. Ganz, A. *et al.* Traction forces exerted through N-cadherin contacts. *Biology of the cell* **98**, 721-730 (2006).
32. Flannery, R.J. & Bruses, J.L. N-cadherin induces partial differentiation of cholinergic presynaptic terminals in heterologous cultures of brainstem neurons and CHO cells. *Frontiers in synaptic neuroscience* **4**, 6 (2012).
33. Bao, J., Jana, S.S. & Adelstein, R.S. Vertebrate nonmuscle myosin II isoforms rescue small interfering RNA-induced defects in COS-7 cell cytokinesis. *The Journal of biological chemistry* **280**, 19594-19599 (2005).
34. Jasaitis, A., Estevez, M., Heysch, J., Ladoux, B. & Dufour, S. E-cadherin-dependent stimulation of traction force at focal adhesions via the Src and PI3K signaling pathways. *Biophysical journal* **103**, 175-184 (2012).

35. Yonemura, S., Wada, Y., Watanabe, T., Nagafuchi, A. & Shibata, M. alpha-Catenin as a tension transducer that induces adherens junction development. *Nature cell biology* **12**, 533-542 (2010).
36. Yao, M. *et al.* Force-dependent conformational switch of alpha-catenin controls vinculin binding. *Nature communications* **5**, 4525 (2014).
37. Choi, H.J. *et al.* alphaE-catenin is an autoinhibited molecule that coactivates vinculin. *Proceedings of the National Academy of Sciences of the United States of America* **109**, 8576-8581 (2012).
38. le Duc, Q. *et al.* Vinculin potentiates E-cadherin mechanosensing and is recruited to actin-anchored sites within adherens junctions in a myosin II-dependent manner. *The Journal of cell biology* **189**, 1107-1115 (2010).
39. Seddiki, R. *et al.* Force-dependent binding of vinculin to alpha-catenin regulates cell-cell contact stability and collective cell behavior. *Molecular biology of the cell* **29**, 380-388 (2018).
40. Smutny, M. *et al.* Myosin II isoforms identify distinct functional modules that support integrity of the epithelial zonula adherens. *Nature cell biology* **12**, 696-702 (2010).
41. Shin, H., Kim, D. & Helfman, D.M. Tropomyosin isoform Tpm2.1 regulates collective and amoeboid cell migration and cell aggregation in breast epithelial cells. *Oncotarget* **8**, 95192-95205 (2017).
42. Caldwell, B.J. *et al.* Tropomyosin isoforms support actomyosin biogenesis to generate contractile tension at the epithelial zonula adherens. *Cytoskeleton (Hoboken, N.J.)* **71**, 663-676 (2014).
43. Han, M.K.L. *et al.* αE-catenin-dependent mechanotransduction is essential for proper convergent extension in zebrafish. *Biology Open* **5**, 1461-1472 (2016).
44. Cai, D. *et al.* Mechanical Feedback through E-Cadherin Promotes Direction Sensing during Collective Cell Migration. *Cell* **157**, 1146-1159 (2014).
45. Buckley, C.D. *et al.* Cell adhesion. The minimal cadherin-catenin complex binds to actin filaments under force. *Science (New York, N.Y.)* **346**, 1254211 (2014).
46. Silvis, M.R. *et al.* alpha-catenin is a tumor suppressor that controls cell accumulation by regulating the localization and activity of the transcriptional coactivator Yap1. *Science signaling* **4**, ra33 (2011).
47. Hirata, H., Samsonov, M. & Sokabe, M. Actomyosin contractility provokes contact inhibition in E-cadherin-ligated keratinocytes. *Scientific reports* **7**, 46326 (2017).
48. Iskratsch, T., Wolfenson, H. & Sheetz, M.P. Appreciating force and shape-the rise of mechanotransduction in cell biology. *Nat Rev Mol Cell Biol* **15**, 825-833 (2014).
49. Thomas, W.A. *et al.* alpha-Catenin and vinculin cooperate to promote high E-cadherin-based adhesion strength. *The Journal of biological chemistry* **288**, 4957-4969 (2013).
50. Benjamin, J.M. *et al.* AlphaE-catenin regulates actin dynamics independently of cadherin-mediated cell-cell adhesion. *The Journal of cell biology* **189**, 339-352 (2010).

51. Sumida, G.M., Tomita, T.M., Shih, W. & Yamada, S. Myosin II activity dependent and independent vinculin recruitment to the sites of E-cadherin-mediated cell-cell adhesion. *BMC cell biology* **12**, 48 (2011).
52. Prager-Khoutorsky, M. *et al.* Fibroblast polarization is a matrix-rigidity-dependent process controlled by focal adhesion mechanosensing. *Nature cell biology* **13**, 1457-1465 (2011).

Figure 1

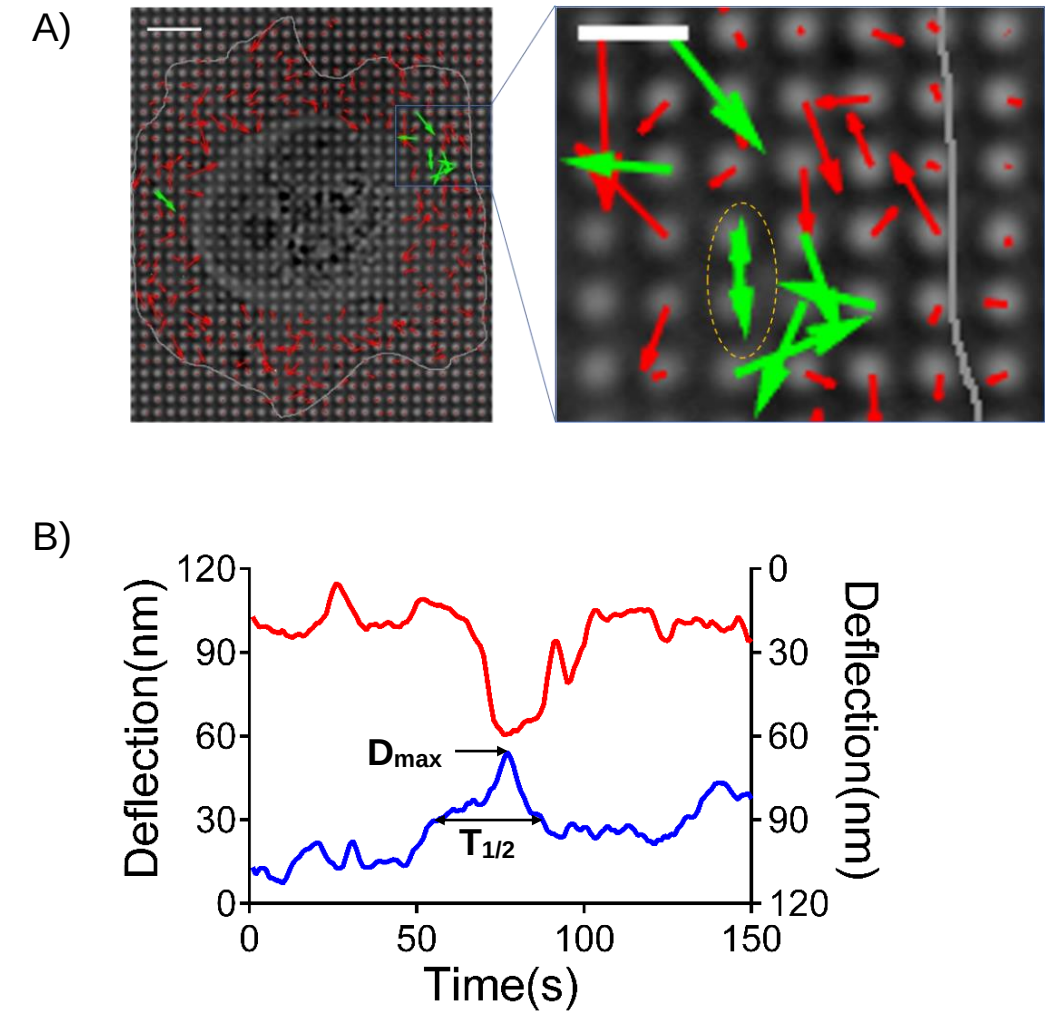

Figure 2

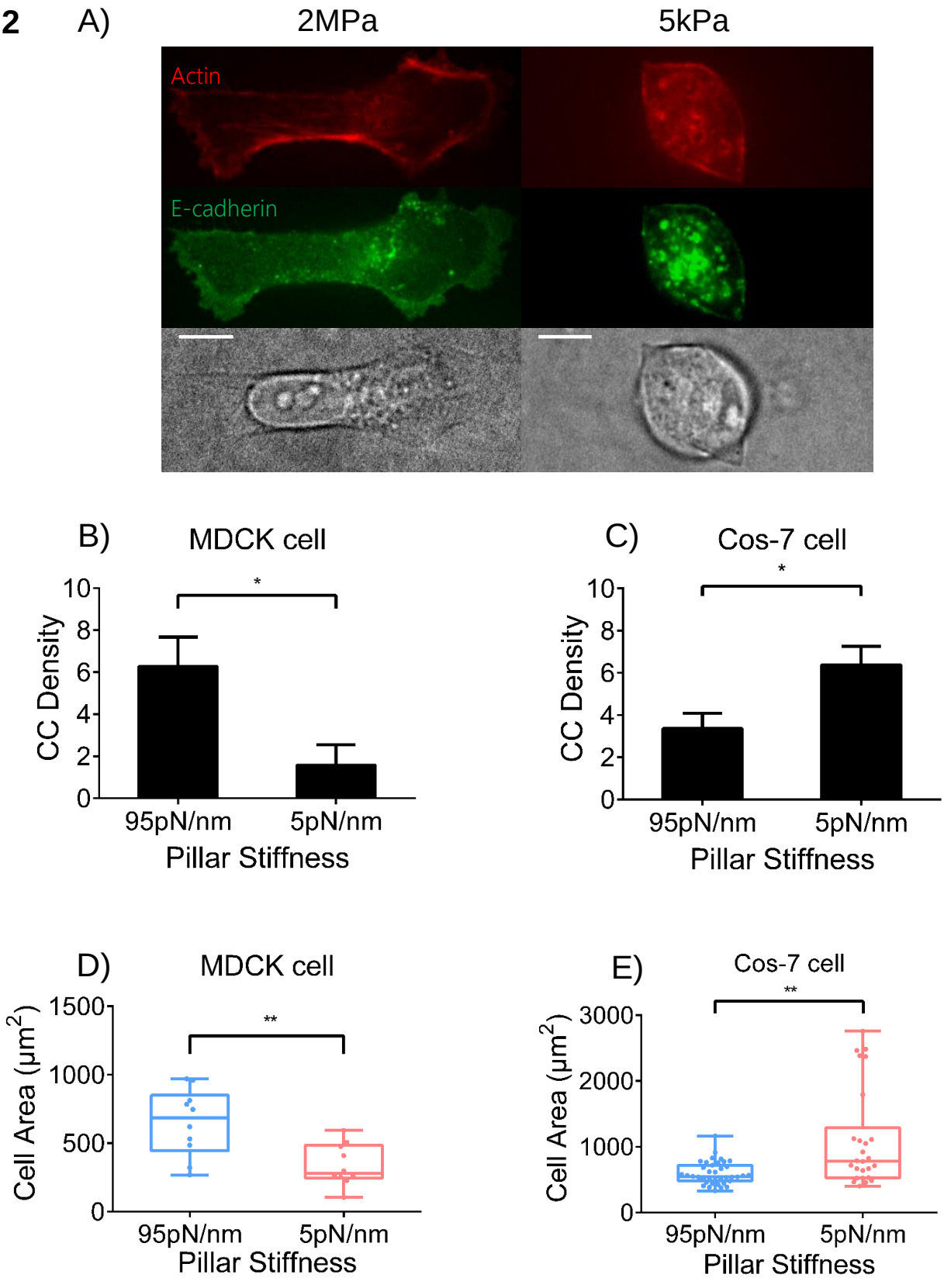

Figure 3

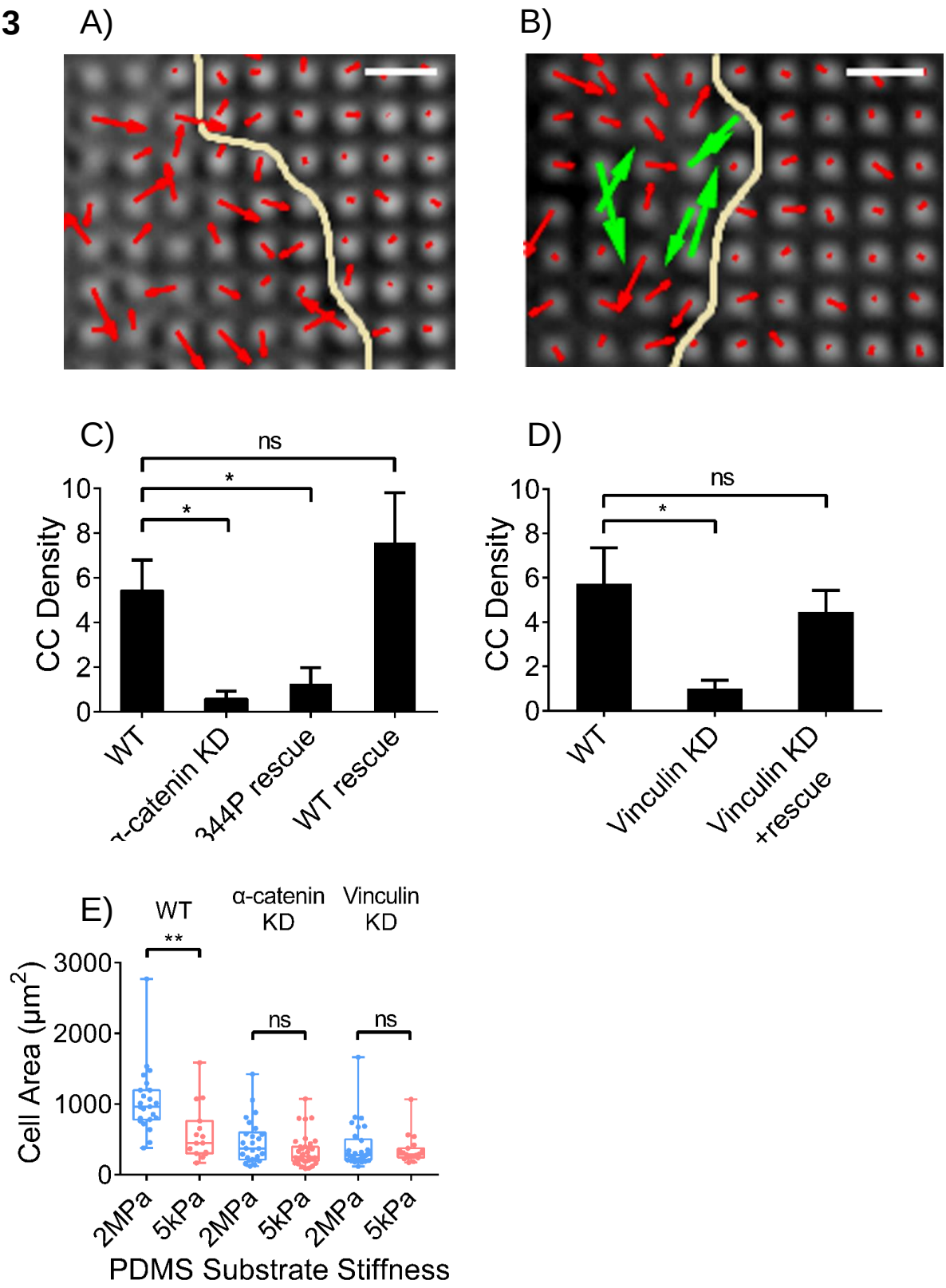

Figure 4

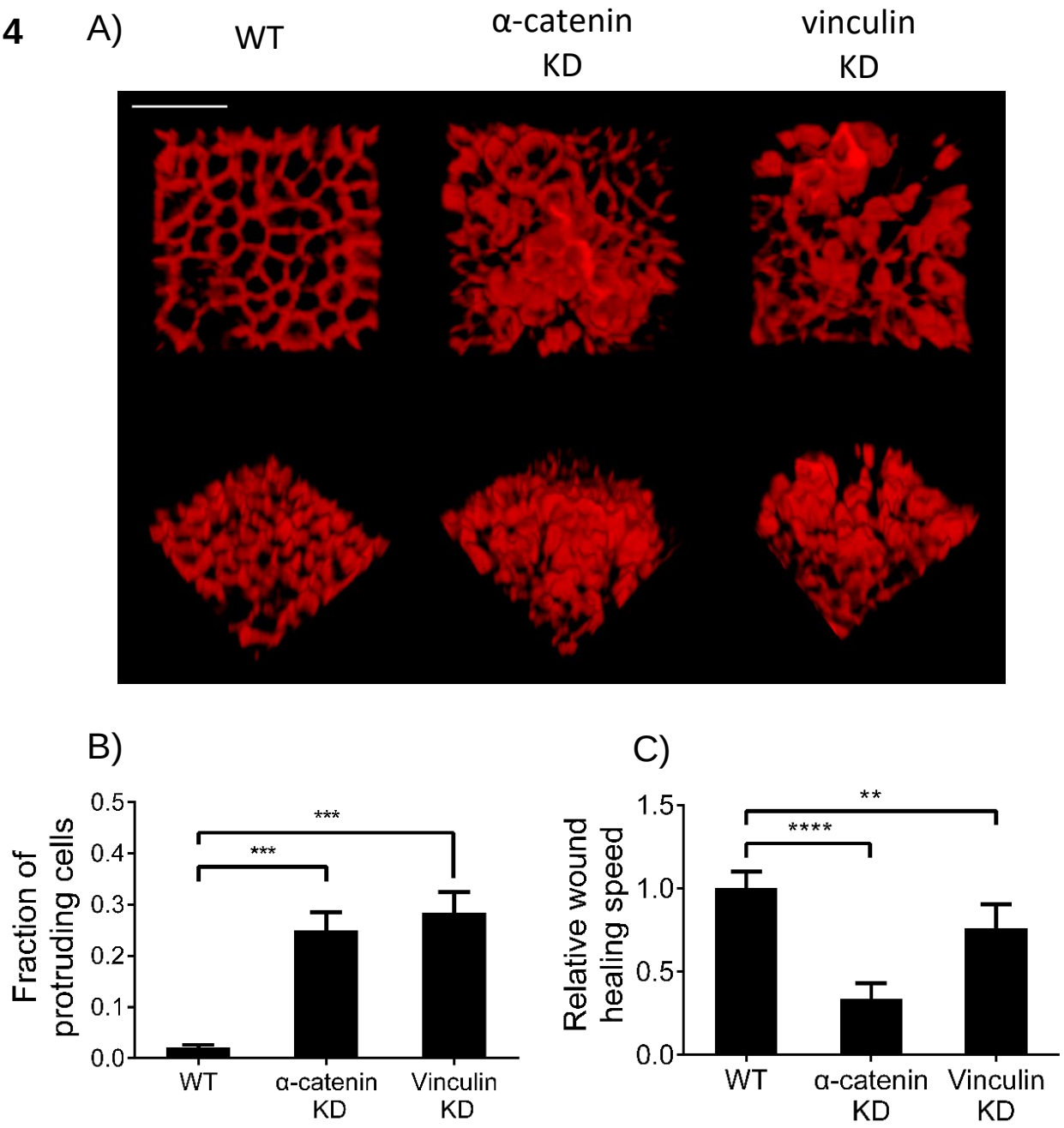

Figure 5

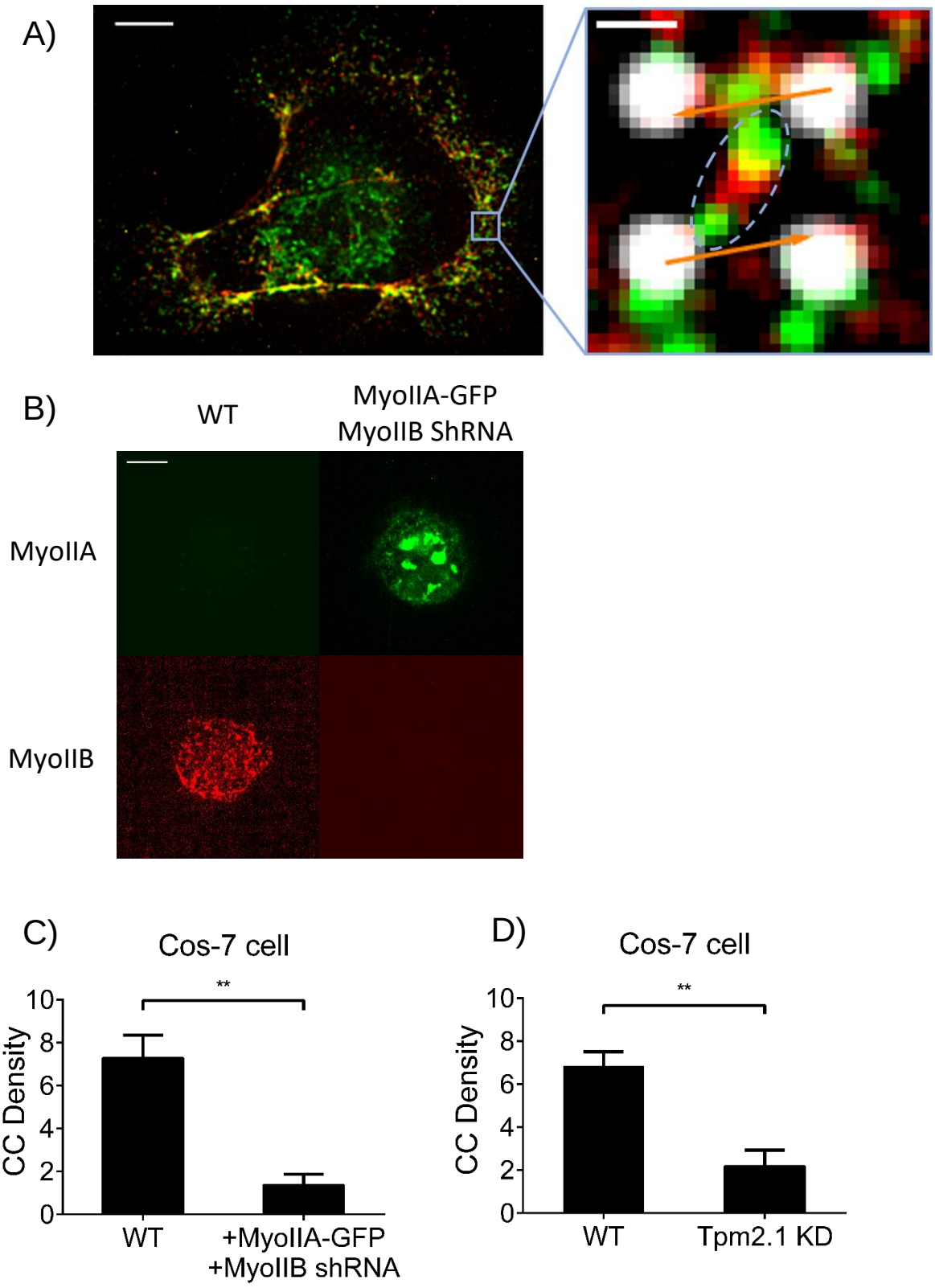

Figure 6